

# Chapter 4

## Gravitational Two-Body Problem

Now we are ready to study what happens when two objects interact via gravity and both are free to move. As we will see, there is a deep connection between the one-body and two-body problems that provides a powerful opportunity to understand binary star systems and extrasolar planets.

### 4.1 Equivalent One-Body Problem

Our first task is to solve the equations of motion and find the orbits in the two-body problem. We can do this by uncovering a mathematical equivalence with the one-body problem, which we have already solved.

#### 4.1.1 Setup

Consider the gravitational interaction between mass  $m_1$  at position  $\mathbf{r}_1$  and mass  $m_2$  at position  $\mathbf{r}_2$ , as sketched in Fig. 4.1. Introducing a few new quantities will clarify our analysis. Define the **separation vector**,

$$\mathbf{r} = \mathbf{r}_2 - \mathbf{r}_1 \quad (4.1)$$

and the **center of mass position**,

$$\mathbf{R} = \frac{m_1\mathbf{r}_1 + m_2\mathbf{r}_2}{m_1 + m_2} \quad (4.2)$$

Also define the **total mass**,

$$M = m_1 + m_2 \quad (4.3)$$

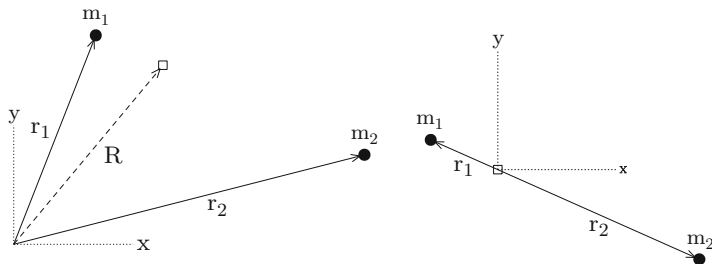


**Fig. 4.1** Geometry of the two-body problem. The *left panel* shows a general reference frame and indicates the vectors to the two objects ( $\mathbf{r}_1$  and  $\mathbf{r}_2$ ) along with the vector to the center of mass ( $\mathbf{R}$ ). The *right panel* shows the reference frame with the center of mass at the origin

and the **reduced mass**,

$$\mu = \frac{m_1 m_2}{m_1 + m_2} \quad \Leftrightarrow \quad \frac{1}{\mu} = \frac{1}{m_1} + \frac{1}{m_2} \quad (4.4)$$

As defined, the total and reduced masses obey the product relation

$$M\mu = m_1 m_2 \quad (4.5)$$

With these definitions, we can rewrite the positions as

$$\mathbf{r}_1 = \mathbf{R} - \frac{\mu}{m_1} \mathbf{r} \quad \text{and} \quad \mathbf{r}_2 = \mathbf{R} + \frac{\mu}{m_2} \mathbf{r} \quad (4.6)$$

Notice that the two objects are *always on opposite sides of the center of mass*. While this should be apparent from the term “center,” it is a good point to keep in mind when visualizing motion in the two-body problem.

Intuitively, the gravitational force on object #1 should point toward object #2, which means the force vector  $\mathbf{F}_1$  is parallel to the separation vector  $\mathbf{r}$ . The force on object #2 points in the opposite direction, so  $\mathbf{F}_2$  has the opposite sign. Newton’s law of gravity tells us that both forces have strength  $Gm_1 m_2 / r^2$ . Putting these pieces together, we can write the forces as

$$\text{force on \#1:} \quad \mathbf{F}_1 = + \frac{Gm_1 m_2}{r^2} \hat{\mathbf{r}} \quad (4.7a)$$

$$\text{force on \#2:} \quad \mathbf{F}_2 = - \frac{Gm_1 m_2}{r^2} \hat{\mathbf{r}} \quad (4.7b)$$

### 4.1.2 Motion

Let’s first consider the acceleration of the center of mass:

$$\frac{d^2\mathbf{R}}{dt^2} = \frac{1}{m_1 + m_2} \left( m_1 \frac{d^2\mathbf{r}_1}{dt^2} + m_2 \frac{d^2\mathbf{r}_2}{dt^2} \right) = \frac{1}{m_1 + m_2} (\mathbf{F}_1 + \mathbf{F}_2) = 0$$

In the first step we replace  $\mathbf{R}$  using Eq. (4.2). In the second step we use Newton's second law to put  $m_i d^2\mathbf{r}_i/dt^2 = \mathbf{F}_i$ , and in the third step we use Newton's third law (in the form of 4.7). We learn that the center of mass does not accelerate.

Therefore we can define an inertial reference with the center of mass at the origin, so  $\mathbf{R} = 0$ . Shifting to this center of mass frame for the remainder of the analysis, we can write

$$\mathbf{r}_1 = -\frac{\mu}{m_1} \mathbf{r} \quad \text{and} \quad \mathbf{r}_2 = \frac{\mu}{m_2} \mathbf{r} \quad (4.8)$$

Note that when we deal with vectors,  $\mathbf{r}_1$  and  $\mathbf{r}_2$  have opposite signs, and the separation vector still includes a minus sign:  $\mathbf{r} = \mathbf{r}_2 - \mathbf{r}_1$ . But if we just consider the *lengths* of vectors, we know the length of the separation vector is (not surprisingly) the sum of the lengths of  $\mathbf{r}_1$  and  $\mathbf{r}_2$ :

$$|\mathbf{r}| = |\mathbf{r}_1| + |\mathbf{r}_2|$$

The ratio of lengths is interesting:

$$\frac{|\mathbf{r}_2|}{|\mathbf{r}_1|} = \frac{m_1}{m_2} \quad (4.9)$$

Even before we fully characterize the motion, we realize that the orbits of the two objects are scaled versions of one another, with the scaling given by the (inverse) mass ratio.

To analyze the motion in detail, consider the equation of motion for object #1:

$$\begin{aligned} m_1 \frac{d^2\mathbf{r}_1}{dt^2} &= \mathbf{F}_1 \\ -\mu \frac{d^2\mathbf{r}}{dt^2} &= \frac{Gm_1m_2}{r^2} \hat{\mathbf{r}} \\ \Rightarrow \frac{d^2\mathbf{r}}{dt^2} &= -\frac{GM}{r^2} \hat{\mathbf{r}} \end{aligned} \quad (4.10)$$

We first use Eq. (4.8) for  $\mathbf{r}_1$  and Eq. (4.7a) for  $\mathbf{F}_1$ , and then use Eq. (4.5) to replace  $m_1m_2$ . Considering object #2 yields the same equation. This equation should look familiar: it is the equation of motion for the gravitational one-body problem. The key lesson is that *a two-body problem with masses  $m_1$  and  $m_2$  is mathematically equivalent to a one-body problem with mass  $M = m_1 + m_2$ .*

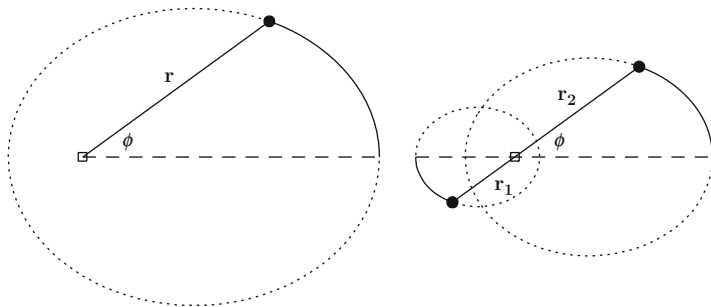


**Fig. 4.2** Sample two-body problem with a 2:1 mass ratio and eccentricity  $e = 0.6$  (*right*) and the equivalent one-body problem (*left*). The two-body orbits are scaled down versions of the one-body ellipse, with the same eccentricity. They share a common focus at the center of mass of the system (denoted by  $\square$ ). As the separation vector sweeps around, it is pinned at the center of mass

We know from Eq. (3.9) that the solution to the one-body problem has the form

$$r = \frac{a(1 - e^2)}{1 + e \cos \phi} \quad (4.11)$$

We can then use Eq. (4.8) to say that the orbits for the two-body problem are smaller ellipses with semimajor axes

$$a_1 = \frac{\mu}{m_1} a \quad \text{and} \quad a_2 = \frac{\mu}{m_2} a \quad (4.12)$$

The orbits are arranged so the two ellipses share a common focus (at the center of mass) and the two objects always lie on opposite sides of the center of mass. The association between a two-body problem and its equivalent one-body analog is illustrated in Fig. 4.2.

As we use the one-body analogy, we need to keep in mind that it is a *mathematical* connection more than a *physical* one. It is not correct to say that a problem with masses  $m_1$  and  $m_2$  orbiting each other is physically equivalent to a problem with masses  $M$  and  $\mu$  orbiting each other. The issue is that a physical scenario with masses  $M$  and  $\mu$  would itself be a two-body problem so both objects would move, but the mathematical equivalence is to a one-body problem in which  $M$  is *stationary*. The analogy between the two-body and one-body problems is powerful, but it must be used with some care.

### 4.1.3 Energy and Angular Momentum

We have seen the analogy with the equation of motion, but does it extend to energy and angular momentum? Let's start with kinetic energy. Equation (4.8) implies that the velocity vectors are related by

$$\mathbf{v}_1 = -\frac{\mu}{m_1} \mathbf{v} \quad \text{and} \quad \mathbf{v}_2 = \frac{\mu}{m_2} \mathbf{v} \quad (4.13)$$

where  $\mathbf{v} = d\mathbf{r}/dt$  is the time derivative of the separation vector. (We are still working in the center of mass frame.) The kinetic energy of each object is then

$$K_i = \frac{1}{2} m_i |\mathbf{v}_i|^2 = \frac{1}{2} \frac{\mu^2}{m_i} |\mathbf{v}|^2$$

The gravitational potential energy between the two objects is

$$U = -\frac{Gm_1m_2}{r} = -\frac{GM\mu}{r}$$

where we use Eq. (4.5). The total energy can therefore be written as

$$\begin{aligned} E &= \frac{1}{2} m_1 |\mathbf{v}_1|^2 + \frac{1}{2} m_2 |\mathbf{v}_2|^2 - \frac{Gm_1m_2}{r} \\ &= \frac{1}{2} \left( \frac{1}{m_1} + \frac{1}{m_2} \right) \mu^2 |\mathbf{v}|^2 - \frac{GM\mu}{r} \\ &= \frac{1}{2} \mu |\mathbf{v}|^2 - \frac{GM\mu}{r} \end{aligned} \quad (4.14)$$

where we use Eq. (4.4) to simplify the first term. A similar analysis of the angular momentum yields

$$\begin{aligned} \mathbf{L} &= m_1 \mathbf{r}_1 \times \mathbf{v}_1 + m_2 \mathbf{r}_2 \times \mathbf{v}_2 \\ &= (\mu \mathbf{r}) \times \left( \frac{\mu \mathbf{v}}{m_1} \right) + (\mu \mathbf{r}) \times \left( \frac{\mu \mathbf{v}}{m_2} \right) \\ &= \left( \frac{1}{m_1} + \frac{1}{m_2} \right) \mu^2 \mathbf{r} \times \mathbf{v} \\ &= \mu \mathbf{r} \times \mathbf{v} \end{aligned} \quad (4.15)$$

The analogy continues to be useful: the final expressions for both energy and angular momentum have forms appropriate for an object of mass  $\mu$  orbiting a (stationary) object of mass  $M$  in a one-body problem.

#### 4.1.4 Velocity Curve

Equation (4.13) gives general relations for the velocity, but it is worthwhile to dig into the details because a lot of what we can learn about binary stars and exoplanets

comes from analyzing velocities. We focus here on  $\mathbf{v}$  for the one-body problem, since  $\mathbf{v}_1$  and  $\mathbf{v}_2$  can be obtained from it. To begin, we find the components of  $\mathbf{v}$  in polar coordinates. The angular component is

$$v_\phi = r \frac{d\phi}{dt} = \frac{\ell}{r} = \frac{\ell(1 + e \cos \phi)}{a(1 - e^2)} \quad (4.16)$$

where we recall that the specific angular momentum  $\ell = r^2 d\phi/dt$  is constant, and we use Eq. (4.11) for  $r$ . The radial component of velocity is

$$v_r = \frac{dr}{dt} = \frac{dr}{d\phi} \frac{d\phi}{dt} = \frac{a(1 - e^2)e \sin \phi}{(1 + e \cos \phi)^2} \frac{d\phi}{dt} = \frac{\ell e \sin \phi}{a(1 - e^2)} \quad (4.17)$$

We use the chain rule to rewrite the derivative, then evaluate  $dr/d\phi$  from Eq. (4.11), and finally substitute for  $d\phi/dt$  using Eq. (4.16). We can convert to Cartesian coordinates as follows:

$$\begin{bmatrix} v_x \\ v_y \end{bmatrix} = \begin{bmatrix} \cos(\phi + \phi_0) & -\sin(\phi + \phi_0) \\ \sin(\phi + \phi_0) & \cos(\phi + \phi_0) \end{bmatrix} \begin{bmatrix} v_r \\ v_\phi \end{bmatrix}$$

where we now allow a general coordinate system in which the major axis of the ellipse lies at angle  $\phi_0$ . Carrying out the matrix multiplication yields

$$v_x = -\frac{\ell[e \sin \phi_0 + \sin(\phi + \phi_0)]}{a(1 - e^2)} \quad \text{and} \quad v_y = \frac{\ell[e \cos \phi_0 + \cos(\phi + \phi_0)]}{a(1 - e^2)} \quad (4.18)$$

To this point we have mainly characterized the orbit as a function of  $\phi$ , and we have not discussed  $\phi(t)$  in much detail. It turns out to be easier to keep  $\phi$  as the independent variable and compute the time dependence as  $t(\phi)$ . Recall from Eq. (3.10) that area in the ellipse is swept out at the rate  $dA/dt = \ell/2$  where  $\ell = \sqrt{GMa(1 - e^2)}$  is the specific angular momentum. If we rewrite this as  $dt = (2/\ell) dA$  and use  $dA = (1/2)r^2 d\phi$  in polar coordinates, we can integrate to obtain

$$t = \frac{1}{\ell} \int r(\phi)^2 d\phi$$

Using  $r(\phi)$  from Eq. (4.11) yields<sup>1</sup>

---

<sup>1</sup>With help from Mathematica [1].

$$\begin{aligned}
 t &= \frac{a^2(1-e^2)^2}{\ell} \int \frac{d\phi}{(1+e \cos \phi)^2} \\
 &= \frac{a^2(1-e^2)^2}{\ell} \left\{ \frac{2}{(1-e^2)^{3/2}} \tan^{-1} \left[ \left( \frac{1-e}{1+e} \right)^{1/2} \tan \frac{\phi}{2} \right] - \frac{e \sin \phi}{(1-e^2)(1+e \cos \phi)} \right\}
 \end{aligned}$$

(We choose the constant of integration so  $t = 0$  at  $\phi = 0$ .) It is convenient to deal with the factor involving  $a$  and  $\ell$  by expressing  $t$  in units of the orbital period,

$$\frac{t}{P} = \frac{1}{2\pi} \left\{ 2 \tan^{-1} \left[ \left( \frac{1-e}{1+e} \right)^{1/2} \tan \frac{\phi}{2} \right] - \frac{e(1-e^2)^{1/2} \sin \phi}{1+e \cos \phi} \right\} \quad (4.19)$$

Note that a circular orbit has  $e = 0$  and hence  $t/P = \phi/2\pi$ , which makes sense.

Now we have the ingredients to understand the shapes of orbits and velocity curves for the two-body problem. Figure 4.3 shows examples with different eccentricities. Recall that the orbits must share a common focus at the center of mass, and the two objects must always lie on opposite sides of this point. If the eccentricity is zero, the orbits are circular and concentric, and the velocity we would measure with the Doppler effect is a sinusoidal function (because it is a projection of circular motion). If the eccentricity is nonzero, the orbit centers are offset from one another, and the velocity curve is less regular. These two effects give us the ability to determine the eccentricity from the shape of the orbits or velocity curves.

### 4.1.5 Application to the Solar System

Let's see how the two-body theory applies to the Solar System and consider whether it was reasonable for Kepler to neglect the Sun's motion. We just want to get a sense of the numbers, so we examine the Sun's interaction with one planet at a time and assume circular orbits for simplicity. For the Sun/Earth system, here are the key quantities:

$$\begin{aligned}
 a &= 1 \text{ AU} = 1.50 \times 10^{11} \text{ m} \\
 P &= 1 \text{ yr} = 3.16 \times 10^7 \text{ s} \\
 m_1 &= 1.99 \times 10^{30} \text{ kg} \\
 m_2 &= 5.97 \times 10^{24} \text{ kg}
 \end{aligned}$$

The corresponding reduced mass is

$$\mu = \frac{m_1 m_2}{m_1 + m_2} = 5.97 \times 10^{24} \text{ kg}$$

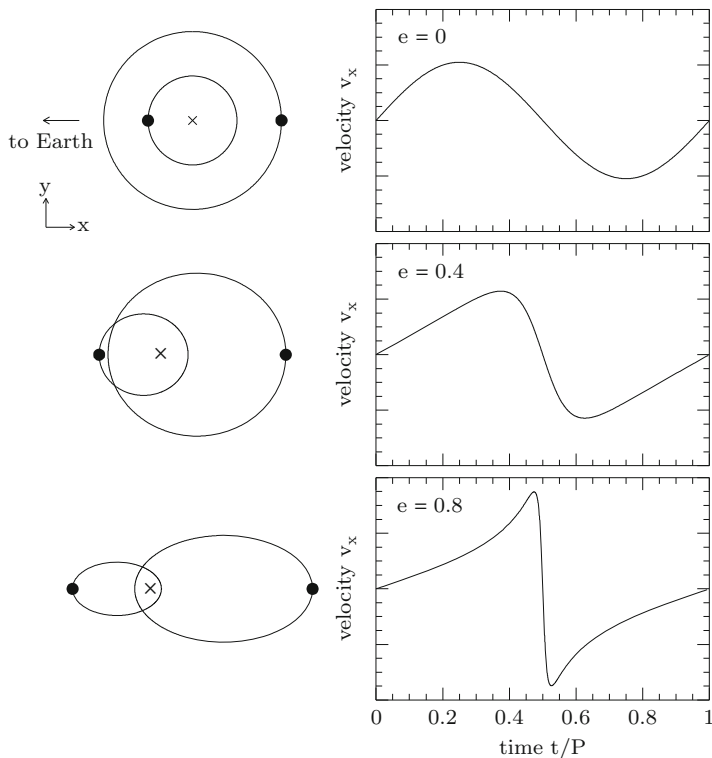


**Fig. 4.3** Examples of two-body orbits and velocity curves. The three rows correspond to different eccentricities. The *left column* shows the orbital configuration, with  $\times$  indicating the center of mass and  $\bullet$  indicating the object positions at  $t = 0$ . The *right column* shows the Doppler velocity we would measure if Earth were off to the left (The observed velocity curve depends on how the orbit is oriented with respect to our line of sight; see Eq. 4.18)

(Note that  $\mu \approx m_2$  when  $m_2 \ll m_1$ .) From Eq. (4.12), the amplitude of the Sun's motion induced by Earth is

$$a_1 = \frac{5.97 \times 10^{24} \text{ kg}}{1.99 \times 10^{30} \text{ kg}} \times 1.50 \times 10^{11} \text{ m} = 4.49 \times 10^5 \text{ m} = 6.5 \times 10^{-4} R_{\odot}$$

The speed of this motion is

$$v_1 = \frac{2\pi a_1}{P} = \frac{2\pi \times (4.49 \times 10^5 \text{ m})}{3.16 \times 10^7 \text{ s}} = 0.089 \text{ m s}^{-1}$$

Since Jupiter is the most massive planet, let's consider it as well:

$$a = 5.20 \text{ AU} = 7.78 \times 10^{11} \text{ m}$$

$$P = 11.86 \text{ yr} = 3.74 \times 10^8 \text{ s}$$

$$m_1 = 1.99 \times 10^{30} \text{ kg}$$

$$m_2 = 1.90 \times 10^{27} \text{ kg}$$

The corresponding reduced mass is

$$\mu = \frac{m_1 m_2}{m_1 + m_2} = 1.90 \times 10^{27} \text{ kg}$$

The amplitude of the Sun's motion induced by Jupiter is

$$a_1 = \frac{1.90 \times 10^{27} \text{ kg}}{1.99 \times 10^{30} \text{ kg}} \times (7.78 \times 10^{11} \text{ m}) = 7.42 \times 10^8 \text{ m} = 1.07 R_{\odot}$$

and the speed of this motion is

$$v_1 = \frac{2\pi \times (7.42 \times 10^8 \text{ m})}{3.74 \times 10^8 \text{ s}} = 12.45 \text{ m s}^{-1}$$

Jupiter affects the Sun more than Earth does, because its larger mass more than compensates for its greater distance.

The Sun's actual motion is more complicated than we have accounted for here, because it is influenced by all objects in the Solar System at once. Even so, the lesson is that the Sun's position changes only by an amount comparable to its size, and its speed is around a dozen meters per second. Such motion was too small for Kepler to detect, which is why he and then Newton could treat planetary motion as a one-body problem.

### 4.1.6 Kepler III Revisited

To conclude our discussion of the theory, let's see how the motion→mass principle applies to the two-body problem. We know from Sect. 3.1 that the equation of motion (4.10) leads to an expression for the orbital period of the form

$$P^2 = \frac{4\pi^2 a^3}{GM}$$

Each object in the two-body system has this same orbital period (they have to stay on opposite sides of the center of mass, after all). Using  $M = m_1 + m_2$  from Eq. (4.3) and  $a = a_1 + a_2$  from Eq. (4.12), we can now write the generalized version of Kepler's third law for two-body problems:

$$P^2 = \frac{4\pi^2(a_1 + a_2)^3}{G(m_1 + m_2)} \quad (4.20)$$

We can still use motion to measure mass in binary systems, but we must understand that what Kepler’s third law gives is *total* mass. In the applications below we will consider if and when it is possible to decompose the total mass into the two individual components.

## 4.2 Binary Stars

Binary systems provide an opportunity to measure accurate masses for stars using two-body theory. We identify three classes of binaries based on what we are able to observe. In a **visual binary**, we can watch the stars move on the sky and follow their orbits. In a **spectroscopic binary**, we can detect absorption lines<sup>2</sup> in the stars’ spectra and use the Doppler effect to measure the velocities along the line of sight. In an **eclipsing binary**, the orbit is nearly edge-on and the stars periodically pass in front of each other. These categories are complementary; any given system may fall into one, two, or all three of them. The way we measure motion is different in each case, so let’s take them one by one and see what we can learn about mass.

### 4.2.1 Background: Inclination

Before we proceed, there is one bit of technical background to discuss. We can observe two dimensions of position projected onto the “plane of the sky,”<sup>3</sup> but the third dimension of distance is often difficult to determine. Even when it can be found, the distance is not precise enough to reveal changes in position along the line of sight. The quantity we can measure along the line of sight is velocity, using the Doppler effect.

This is an issue for binary stars because the orbital plane can have an arbitrary orientation with respect to the line of sight. We define the inclination angle  $i$  to be the angle between the orbital plane and the plane of the sky, as shown in Fig. 4.4. To be more precise, let  $\hat{\mathbf{n}}$  be a unit vector perpendicular to the orbital plane, which we call the **normal vector**. The inclination is the angle between the normal vector and the line of sight; this is the same as the polar angle  $\theta$  if we express  $\hat{\mathbf{n}}$  in spherical

---

<sup>2</sup>In Chap. 14 we study spectral lines created by atoms and molecules in the outer layers of stars.

<sup>3</sup>Strictly speaking, we measure angles on the spherical sky. If the angular extent of a system is small, we can project onto a plane tangent to the sphere to obtain Euclidean coordinates without making a significant error.

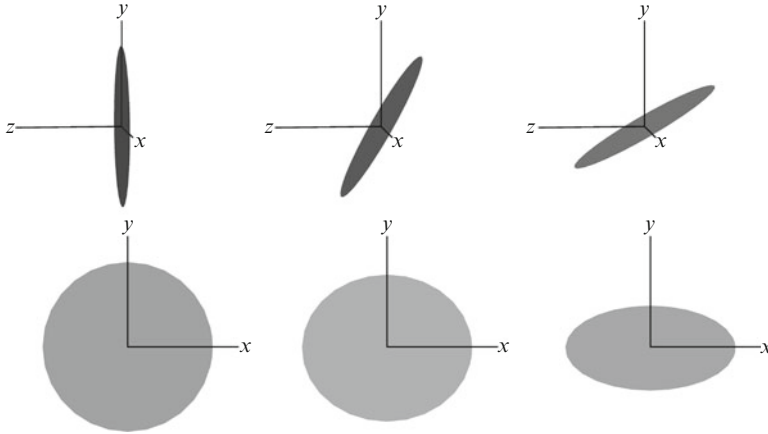


**Fig. 4.4** Illustration of inclination. The *top row* shows nearly side-on views, while the *bottom row* shows the corresponding face-on views (looking down the  $z$ -axis). The columns display different inclinations:  $i = 0^\circ$  (*left*),  $i = 30^\circ$  (*middle*), and  $i = 60^\circ$  (*right*)

coordinates. With this definition, a face-on orbit has  $i = 0^\circ$  while an edge-on orbit has  $i = 90^\circ$ .

To specify what we can measure, let  $(x_{\text{int}}, y_{\text{int}}, z_{\text{int}})$  be the intrinsic coordinate system in which the orbital motion is in the  $(x_{\text{int}}, y_{\text{int}})$ -plane, while  $(x_{\text{obs}}, y_{\text{obs}}, z_{\text{obs}})$  is the observed coordinate system in which we are looking along the  $z_{\text{obs}}$ -axis. The two frames are rotated with respect to one another by the angle  $i$ . Let's choose coordinates so the  $x$ -axes line up and the rotation applies to the  $y$ - and  $z$ -directions. Then the observed position is related to the intrinsic position by

$$x_{\text{obs}} = x_{\text{int}} \quad \text{and} \quad y_{\text{obs}} = y_{\text{int}} \cos i \tag{4.21}$$

(Recall that the intrinsic orbital motion has  $z_{\text{int}} = 0$ .) The measured velocity along the line of sight is

$$v_{z,\text{obs}} = v_{y,\text{int}} \sin i \tag{4.22}$$

The factors of  $\cos i$  and  $\sin i$  will be important in what follows. For each type of binary system, we need to consider whether the inclination can be determined, and how it affects our analysis.

Inclination can run between  $0^\circ$  and  $90^\circ$ , but the values are not all equally likely. If orientations are random in space, the normal vector will be distributed uniformly over the unit sphere. Figure 4.5 shows that there is more area on the sphere with a larger value of  $i$ , and less area with a smaller value of  $i$ . In fact, the area is such that the probability distribution for inclination is

$$p(i) = \sin i \tag{4.23}$$

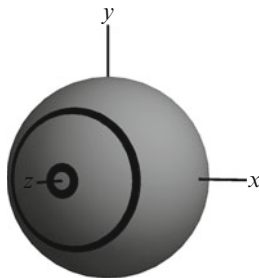


**Fig. 4.5** If orbital orientations are random, the normal vector will be distributed uniformly over the unit sphere. The *small black band* indicates the set of normal vectors that correspond to inclinations in the range  $5^\circ < i < 10^\circ$ , while the large band has  $40^\circ < i < 45^\circ$ . Larger inclinations have a higher probability of being seen, with  $p(i) = \sin i$

This factor of  $\sin i$  is the same as the factor of  $\sin \theta$  in the spherical coordinate volume element,  $dV = r^2 \sin \theta dr d\theta d\phi$ .

### 4.2.2 Visual Binary

If we can see both stars and watch them move, we can measure the period and trace the orbits directly. Can we determine the inclination? This might seem tricky at first because inclination causes an orbit to look squashed (due to the  $\cos i$  factor in Eq. 4.21): a circle can look like an ellipse, or an ellipse can look more flattened than it truly is. There is, however, an important distinction between the configuration of orbits in a system with inclined circular orbits and a system with face-on elliptical orbits, as you can understand through Problem 4.1. The analysis is a little more subtle when the orbits are both elliptical and inclined, but the key idea is that the *true* orbits must satisfy Kepler's laws while the *projected* orbits may not. This principle makes it possible to deduce the true orbits and hence determine the inclination.

The challenge with visual binaries is that we can only measure the *angular* size of the orbits. If  $\alpha_1$  and  $\alpha_2$  are the angles subtended by the semimajor axes of the orbits, the corresponding physical lengths are

$$a_i = D \tan \alpha_i \approx D\alpha_i$$

where  $D$  is the distance to the binary system, and we are using the small-angle approximation  $\tan \alpha_i \approx \alpha_i$ . We can still find the mass ratio using Eq. (4.9):  $m_2/m_1 = a_1/a_2 = \alpha_1/\alpha_2$ . But if we want to find the actual masses using Eq. (4.20), we need to know the distance:

$$m_1 + m_2 = \frac{4\pi^2 D^3 (\alpha_1 + \alpha_2)^3}{GP^2}$$

Inclination is not a problem for visual binaries, but distance is.

### 4.2.3 Spectroscopic Binary

If a binary system is too distant and/or small, we may not be able to resolve the two stars on the sky. We can still analyze the motion, though, by using spectroscopy. As the stars move in their orbits, the Doppler effect causes each star's spectral lines to shift to shorter wavelengths when the star is moving toward us, and to longer wavelengths when the star is moving away.

#### Double-Line System

If we see distinct spectral lines from both stars, we can measure both of the Doppler velocity curves. The amplitude of the velocity curve for star #1 can be found by using Eqs. (4.13) and (4.18) for the intrinsic velocity and including a factor of  $\sin i$  from projection (Eq. 4.22):

$$k_1 = \frac{\mu}{m_1} \frac{\ell}{a(1-e^2)} \sin i = \frac{\mu}{m_1} \frac{2\pi a}{P(1-e^2)^{1/2}} \sin i$$

where we simplify using Eqs. (3.11) and (4.20). The expression for  $k_2$  is similar, with  $m_2$  replacing  $m_1$ . If we measure both velocity amplitudes and take the ratio, most of the factors drop out,

$$\frac{k_2}{k_1} = \frac{m_1}{m_2} \quad (4.24)$$

and we can determine the ratio of masses directly from the measurements. Also, if we add the velocity amplitudes we find:

$$k_1 + k_2 = \mu \left( \frac{1}{m_1} + \frac{1}{m_2} \right) \frac{2\pi a}{P(1-e^2)^{1/2}} \sin i = \frac{2\pi a}{P(1-e^2)^{1/2}} \sin i$$

where we use Eq. (4.4) to simplify. Thus, we can write the semimajor axis in terms of the measurable<sup>4</sup> quantities  $k_1$ ,  $k_2$ ,  $P$ , and  $e$  as

$$a = \frac{P(1-e^2)^{1/2}}{2\pi} \frac{k_1 + k_2}{\sin i} \quad (4.25)$$

Using this in Kepler's third law gives the total mass as

$$m_1 + m_2 = \frac{P(1-e^2)^{3/2}}{2\pi G} \left( \frac{k_1 + k_2}{\sin i} \right)^3 \quad (4.26)$$

---

<sup>4</sup>Recall from Sect. 4.1.4 that we can determine  $e$  from the shape of the velocity curves.

For a spectroscopic binary, we can measure the absolute masses only if we know  $i$ . That makes spectroscopic binaries the opposite of visual binaries in the sense that distance is not a problem, but inclination is. If the inclination is unknown, the observables determine only the products  $m_1 \sin^3 i$  and  $m_2 \sin^3 i$ .

### Single-Line System

If one object (say, star #2) is faint, we may not be able to detect its absorption lines in the spectrum. We can still use the wavelength oscillations of the lines we do see to deduce that star #1 is in a binary orbit, and to measure its velocity amplitude  $k_1$  as well as the orbital period  $P$  and eccentricity  $e$ . Now what can we do? Let's go back to Eq. (4.26) and use Eq. (4.24) to eliminate  $k_2$ , since it is not measurable:

$$m_1 + m_2 = \frac{P(1-e^2)^{3/2}}{2\pi G} \left( \frac{k_1 + k_1 m_1/m_2}{\sin i} \right)^3 = \frac{P(1-e^2)^{3/2}}{2\pi G} \left( \frac{k_1}{\sin i} \frac{m_2 + m_1}{m_2} \right)^3$$

Rearranging yields

$$\frac{m_2 \sin i}{(m_1 + m_2)^{2/3}} = \left( \frac{P}{2\pi G} \right)^{1/3} (1 - e^2)^{1/2} k_1 \quad (4.27)$$

In other words, we can use the observables to infer a funny combination of masses, along with the usual inclination factor.

What good is this? Let's make two assumptions. First, suppose  $m_2 \ll m_1$  so the left-hand side is approximately

$$\frac{m_2 \sin i}{m_1^{2/3}}$$

Second, suppose we have some way to estimate  $m_1$  (perhaps from other properties of the star, such as its brightness and color). Then we can move  $m_1$  to the right-hand side in Eq. (4.27) and write

$$m_2 \sin i = \left( \frac{m_1^2 P}{2\pi G} \right)^{1/3} (1 - e^2)^{1/2} k_1 \quad (4.28)$$

As we will see in Sect. 4.3, these two assumptions are reasonable for extrasolar planets, so measuring Doppler velocities of stars lets us determine  $m_2 \sin i$  for planets orbiting those stars.

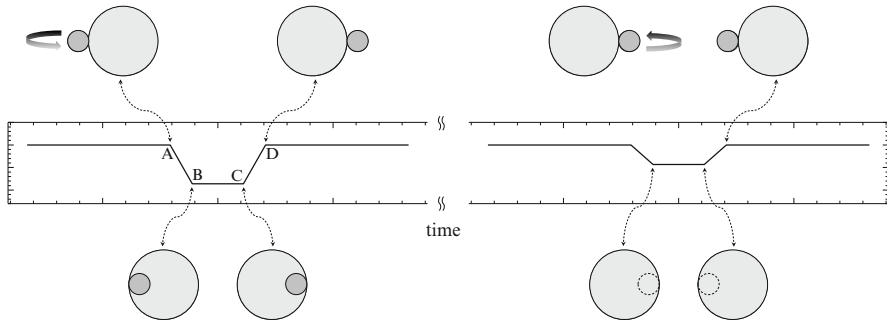


**Fig. 4.6** Schematic light curve for an eclipsing binary, and the corresponding star configurations. (*Left*) During the primary eclipse, the small star is coming out of the page and moving left-to-right in front of the large star. (*Right*) During the secondary eclipse, the small star is going into the page and moving right-to-left behind the large star. In this example, the large star has a higher surface brightness (luminosity per unit area) than the small star

#### 4.2.4 Eclipsing Binary

If a binary system is very close to edge-on, one star can fully or partially eclipse the other. The **light curve**, or brightness as a function of time, will dip during the eclipse events as shown in Fig. 4.6. Eclipses can occur only if  $i \approx 90^\circ$  (or  $\sin i \approx 1$ ), so seeing them solves the inclination problem in spectroscopic binaries and lets us determine the absolute masses of the two stars.

Eclipses contain information about the *sizes* of stars as well. In Sect. 4.3.2, we will see that eclipse depth alone can reveal the relative sizes of the stars (or, in the case below, a star and a planet). If we combine eclipses with Doppler velocities, we can go a step further and determine the absolute sizes. For example, the time between points A and B in Fig. 4.6 is the time it takes for the stars to move (relative to one another) by the diameter of the small star. Since the stars are moving in opposite directions, their relative speed is  $v_1 + v_2$ . The radius of the smaller star is therefore

$$R_{\text{small}} = \frac{1}{2}(v_1 + v_2)(t_B - t_A)$$

(How would you determine the radius of the larger star?)

### 4.3 Extrasolar Planets

Since 1995, hundreds of planets have been discovered around other stars using the techniques we just discussed. A star+planet system acts as a single-line spectroscopic binary, while an edge-on system acts as an eclipsing binary. The effects

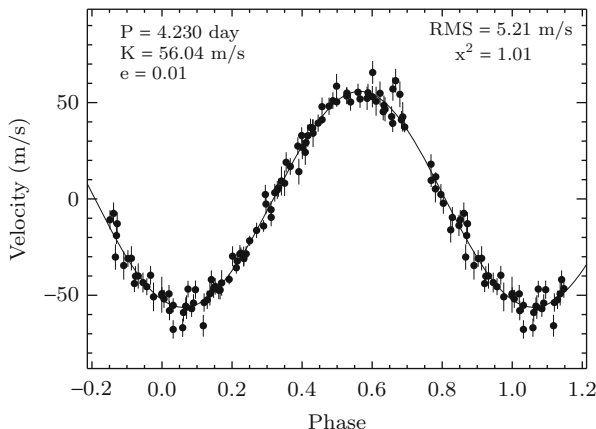


**Fig. 4.7** Radial velocity curve for the star 51 Peg, where  $\phi$  denotes orbital phase (Credit: Marcy et al. [2]. Reproduced by permission of the AAS (Also see Mayor et al. [3]))

are generally small—speeds are typically tens of meters per second or smaller, and eclipse depths are at the percent level or smaller—but they can now be measured routinely. Systems in which we can measure both motion and eclipses are particularly valuable, as we will see.

### 4.3.1 Doppler Planets

A star with a planet is a prime example of a single-line spectroscopic binary; the planet contributes very little light to the spectrum, so it does not introduce detectable absorption lines, but its gravity causes the star to “wobble” so the spectral lines oscillate in wavelength. As we saw in Eq. (4.28), if the planet is much less massive than the star then we can estimate  $m_2 \sin i$ , but we need to know the mass of the star. This can be often inferred from the star’s visible properties; as we will see in Chap. 16, there are good relations between the mass, luminosity, color, and spectroscopic properties of stars.

The first extrasolar planet discovered orbits the star 51 Peg [3]. Figure 4.7 shows that the star’s velocity curve is nearly sinusoidal, indicating that the orbit is close to circular. The measured period, eccentricity, and velocity amplitude are [4]

$$P = 4.23 \text{ day} = 3.65 \times 10^5 \text{ s}$$

$$e = 0.013$$

$$k_1 = 55.9 \text{ m s}^{-1}$$

The mass of the star is estimated to be  $m_1 = 1.05 M_\odot = 2.09 \times 10^{30}$  kg. Using these values in Eq. (4.28) yields for the planet:

$$\begin{aligned} m_2 \sin i &= \left[ \frac{(2.09 \times 10^{30} \text{ kg})^2 \times (3.65 \times 10^5 \text{ s})}{2\pi \times (6.67 \times 10^{-11} \text{ m}^3 \text{ kg}^{-1} \text{ s}^{-2})} \right]^{1/3} (1 - 0.013^2)^{1/2} \times 55.9 \text{ m s}^{-1} \\ &= 8.73 \times 10^{26} \text{ kg} \\ &= 0.46 M_J \end{aligned}$$

So  $m_2 \sin i$  is comparable to the mass of Jupiter and much smaller than the mass of a typical star. Does that automatically imply that  $m_2$  itself is small, i.e., that the second object is a planet? The alternative is that  $i$  is small, i.e., that the second object is a star but the orbits are very close to face-on. The early phase of exoplanet studies faced this key question: do low values of  $m_2 \sin i$  indicate planets or just binary star systems in nearly face-on orbits?

One way to proceed is to make a statistical argument and point out that only a small fraction of orbits are nearly face-on. If observed  $m_2 \sin i$  values are small because  $m_2$  is large but  $i$  is small, then we would expect there to be many other systems where  $i$  and hence  $m_2 \sin i$  are larger. How many? In order for us to misinterpret a stellar companion with mass  $M_s$  as a planet less massive than Jupiter, we would need

$$M_s \sin i \leq M_J \quad \Rightarrow \quad i \leq \sin^{-1} \left( \frac{M_J}{M_s} \right)$$

The probability for this to occur is

$$\text{Pr} = \int_0^{\sin^{-1}(M_J/M_s)} p(i) \, di$$

where  $p(i) = \sin i$  from Eq. (4.23). If there are  $N_{\text{tot}}$  systems overall, and  $N_J$  systems in which we think the companion is a planet less massive than Jupiter, then  $N_J/N_{\text{tot}}$  is given by this probability. Therefore we can compute

$$\begin{aligned} \frac{N_J}{N_{\text{tot}}} &= \int_0^{\sin^{-1}(M_J/M_s)} \sin i \, di \\ &= 1 - \cos \left( \sin^{-1} \frac{M_J}{M_s} \right) \\ &= 1 - \sqrt{1 - \left( \frac{M_J}{M_s} \right)^2} \\ &\approx \frac{M_J^2}{2M_s^2} \end{aligned}$$

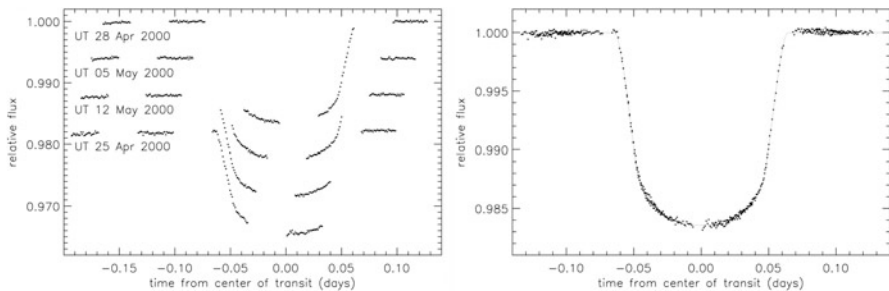


**Fig. 4.8** Transit light curve for HD 209458, from Hubble Space Telescope observations. The *left panel* shows four individual eclipses (vertically offset for clarity), while the *right panel* shows all events superimposed (Credit: Brown et al. [7]. Reproduced by permission of the AAS)

where in the last step we make a Taylor series expansion assuming  $M_J \ll M_s$ . If the true companion mass were  $M_s = M_\odot$ , then we would expect  $N_{\text{tot}}/N_J = 2.2 \times 10^6$ , or more than a million times as many “stellar” companions as “planetary” companions. Even if the true companion mass were as low as  $M_s = 0.08 M_\odot$  (which is the smallest mass we consider to be a star; see Chap. 16), we would still expect  $N_{\text{tot}}/N_J = 14,000$ . In other words, if systems like 51 Peg were really stellar binaries seen nearly face-on, there ought to be many more systems seen at moderate inclinations with larger values of  $m_2 \sin i$ . The statistics suggested otherwise, but the argument was indirect and did not actually prove that the objects are planets.

### 4.3.2 Transiting Planets

Strong confirmation that some companions are in fact planets came with the discovery of planets that cross in front of their stars and produce eclipsing binaries. As we noted in Sect. 4.2.4, seeing a transit proves that a system is very close to edge-on, so  $\sin i \approx 1$  and  $m_2 \sin i$  accurately represents the companion’s mass.

The first transiting planet found orbits a star called HD 209458 [5,6]. The eclipse light curve, shown in Fig. 4.8, is more complicated than the simple flat-bottomed curve sketched in Fig. 4.6. Previously we assumed the star was a flat, uniformly-bright disk, but in fact it is a sphere emitting light isotropically and we receive more light from the part of the surface that faces us and less light from the limbs. This

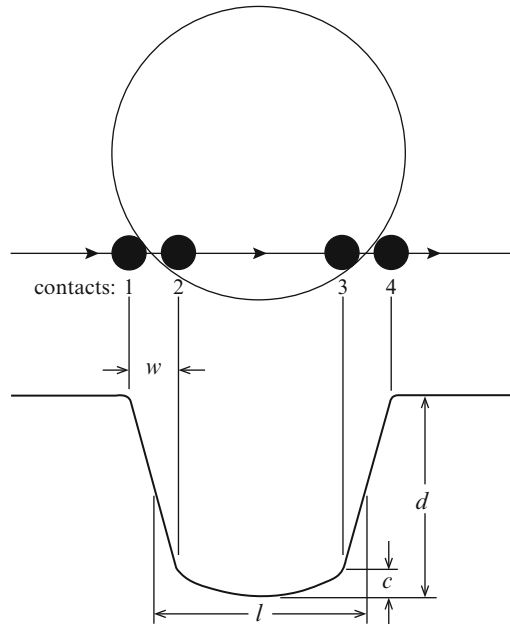


**Fig. 4.9** Schematic diagram of the HD 209458 eclipse (Credit: Brown et al. [7]. Reproduced by permission of the AAS)

“limb darkening” effect can be incorporated into detailed models of the eclipse, leading to the picture shown in Fig. 4.9.

Transits reveal the size of the planet, with the simplest analysis using just the depth of the eclipse. The planet blocks a fraction of the star’s visible area given by

$$f_{\text{ecl}} = \frac{\pi R_2^2}{\pi R_1^2} = \left(\frac{R_2}{R_1}\right)^2$$

where  $R_1$  and  $R_2$  are the radii of the star and planet, respectively. If we assume the star is a uniform disk (again, not correct but reasonable for a simple estimate), then  $f_{\text{ecl}}$  is also the fraction of the star’s light that is blocked during the eclipse. Once we see an eclipse, we can use the depth to measure the size of the planet in relation to the size of the star. Then with an independent estimate of the star’s size we can determine the planet’s actual size, which we can finally combine with the mass to estimate the density. This is a big step toward understanding the physical properties and compositions of exoplanets.

### Application to HD 209458

Let's examine the numbers for HD 209458b<sup>5</sup> [8]. This is a system with both Doppler and transit information, so we can use a joint analysis to learn a lot about the planet. The star's mass and radius are estimated to be

$$\begin{aligned} m_1 &= 1.13 M_\odot = 2.25 \times 10^{30} \text{ kg} \\ R_1 &= 1.16 R_\odot = 8.07 \times 10^8 \text{ m} \end{aligned}$$

The orbital period and velocity amplitude for the star's motion are

$$\begin{aligned} P &= 3.52 \text{ day} = 3.04 \times 10^5 \text{ s} \\ k_1 &= 84.7 \text{ m s}^{-1} \end{aligned}$$

(The orbital eccentricity is small and assumed to be 0.) From the motion we can compute the mass of the companion:

$$\begin{aligned} m_2 &= \left[ \frac{(2.25 \times 10^{30} \text{ kg})^2 \times (3.04 \times 10^5 \text{ s})}{2\pi \times (6.67 \times 10^{-11} \text{ m}^3 \text{ kg}^{-1} \text{ s}^{-2})} \right]^{1/3} \times 84.7 \text{ m s}^{-1} \\ &= 1.31 \times 10^{27} \text{ kg} \\ &= 0.69 M_J \end{aligned}$$

where we use  $\sin i \approx 1$ . Also, rearranging Kepler's third law and approximating  $m_1 + m_2 \approx m_1$  lets us find the semimajor axis, which is the distance of the planet from the star:

$$\begin{aligned} a &\approx \left( \frac{Gm_1 P^2}{4\pi^2} \right)^{1/3} \\ &\approx \left[ \frac{(6.67 \times 10^{-11} \text{ m}^3 \text{ kg}^{-1} \text{ s}^{-2}) \times (2.25 \times 10^{30} \text{ kg}) \times (3.04 \times 10^5 \text{ s})^2}{4\pi^2} \right]^{1/3} \\ &\approx 7.06 \times 10^9 \text{ m} \\ &\approx 0.047 \text{ AU} \end{aligned}$$

---

<sup>5</sup>By convention, planets are named by appending letters starting with "b" to the name of the star. For example, HD 209458b is a planet orbiting the star HD 209458.

The eclipse depth is 1.46 %, so the planet’s size relative to the star is estimated to be

$$\frac{R_2}{R_1} = (0.0146)^{1/2} = 0.12$$

Factoring in the star’s size yields for the planet:

$$R_2 = 9.8 \times 10^7 \text{ m} = 1.4 R_J$$

Now combining the mass and radius lets us compute the mean density<sup>6</sup>

$$\rho_2 = \frac{3m_2}{4\pi R_2^3} = 340 \text{ kg m}^{-3} = 0.34 \text{ g cm}^{-3}$$

There are many things to say:

- The planet is roughly the mass and size of Jupiter, but is very close to its star.
- The density is much less than that of water, so the planet must be gaseous (as opposed to a rocky world like Earth).
- The planet is less massive but larger than Jupiter. It appears to be “puffed up” compared to Jupiter, presumably by heat from its star.

The discovery of large, massive planets very close to their stars—planets now called **hot Jupiters**—came as an enormous surprise and posed a significant challenge to theories of planet formation. In the traditional picture, which we will examine in Sect. 19.4.2, planets close to a star are expected to be rocky (like the terrestrial planets Mercury, Venus, Earth, and Mars in our Solar System) because it was too hot near the star for planetesimals to accumulate much gas or ice. Only planets forming farther from the star were able to collect volatile elements and grow much bigger. It seems difficult to change that picture, so the idea has emerged that hot Jupiters formed much farther from their stars than they are now, and then **migrated** inwards. Understanding how this migration occurred is a hot topic (pardon the pun) in planet formation theory.

### 4.3.3 Status of Exoplanet Research

Studies of exoplanets are advancing at an amazing rate. As of December 2013, more than 400 planets have been detected by the Doppler technique. With sensitive spectrographs it is now possible to measure star velocities as small as  $0.25 \text{ m s}^{-1}$

---

<sup>6</sup>We follow common practice and quote planet densities in CGS rather than MKS units because densities are of order unity in  $\text{g cm}^{-3}$ . For example, water has a density of  $1 \text{ g cm}^{-3}$  at standard temperature and pressure on Earth, while rocks and metals have densities of several  $\text{g cm}^{-3}$ . Earth’s average density is about  $5.5 \text{ g cm}^{-3}$ .

and thus to find planets with  $m \sin i$  values comparable to the mass of Earth [9]. Well-measured velocity curves can reveal complicated motion caused by multiple planets; the most populous Doppler system found so far has at least five and perhaps as many as seven planets [10]. At the same time, more than 250 planets have been detected by the transit technique, along with some 2,500 more candidates from the Kepler mission. Kepler’s precise transit measurements make it possible to discover planets as small as Mercury [11], systems with as many as six planets [12], and even planets orbiting binary stars [13, 14]. (Another technique for finding planets is based on gravitational microlensing, which we will discuss in Sect. 9.2.4.)

After finding planets, the next step is to characterize their physical properties. As we saw with HD 209458b, measuring both mass and radius lets us use the mean density to investigate the bulk composition. There seems to be a lot of diversity: for example, the planet Kepler-10b has a mass of  $4.6 M_{\oplus}$  and a density of  $8.8 \text{ g cm}^{-3}$ , suggesting that it is made of rock and metals [15], while Kepler-11e has a mass of  $8.0 M_{\oplus}$  and a density of  $0.58 \text{ g cm}^{-3}$ , suggesting that it has a significant amount of light gas such as hydrogen and helium [12].

With transiting hot Jupiters we can investigate planetary atmospheres in some detail.<sup>7</sup> For example, spectra taking during a transit can reveal absorption by atoms and molecules when the star’s light passes through the planet’s atmosphere [16]. Infrared observations are sensitive to light *emitted* by hot planets. Most of time we receive light from both the star and planet, but during the secondary eclipse (when the planet goes behind the star; see Fig. 4.6) we receive light only from the star; we can use the difference to determine the brightness and temperature of the planet. We can even measure differences between daytime and nighttime temperatures and then investigate how effectively winds and clouds distribute heat across the planet [17, 18]. (For a more comprehensive review of work on exoplanet atmospheres, see [19].)

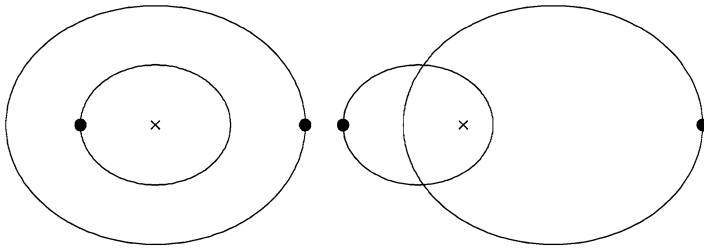
There is broad interest in finding planets similar to Earth. We could think about similarity in terms of mass, size, composition, etc., but perhaps the most tantalizing aspect is the ability to host life. On Earth it seems that liquid water is important for life, so we typically define the “habitable zone” around a star to be the region in which water could exist in liquid form (see Chap. 13, especially Problem 13.7). Kepler has found several planets that lie in the habitable zone and are between 40 and 140 % larger than Earth [20–22]. Their compositions are not known so it remains to be seen whether these planets are like Earth, Venus, or something altogether different. Nevertheless, it is remarkable to see how far exoplanet research has advanced in less than two decades since 51 Peg b was discovered—and to think that it all rests on the foundation of the gravitational two-body problem.

---

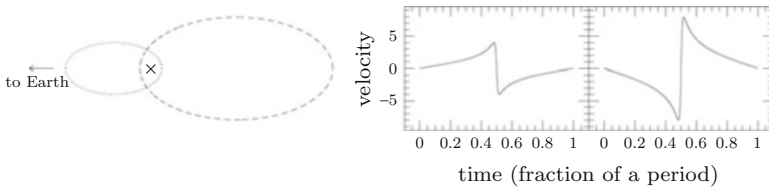
<sup>7</sup>We defer our own study of atmospheric physics to Chaps. 12 and 13; here we briefly summarize recent work on exoplanets.

### Problems

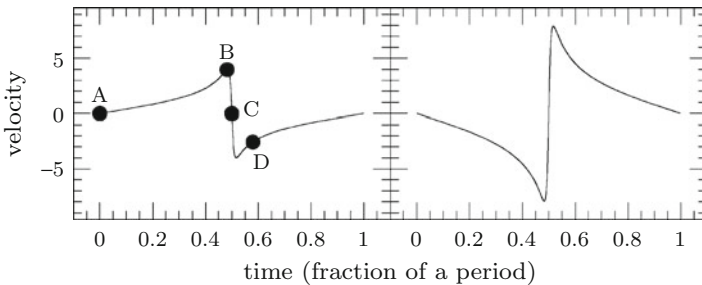
4.1. Imagine that we see two visual binary systems with the orbits shown below (× denotes the center of mass). One represents a system with elongated orbits viewed face-on, while the other represents a system with circular orbits that are inclined to our line of sight. How can you determine which is which?



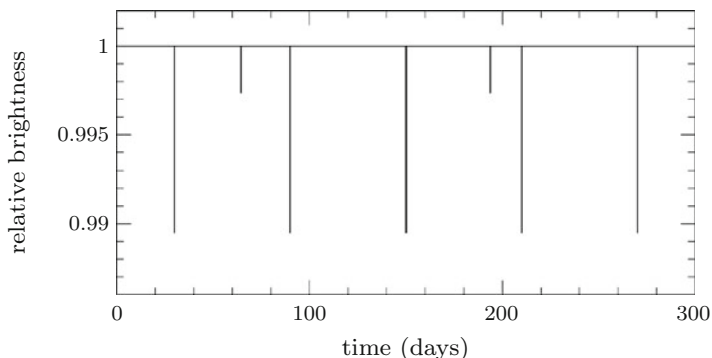
4.2. Here are the orbits of two stars in a binary system, along with Doppler velocity curves measured by an observer off to the left and in the plane of the orbits. (The velocity units are not important for this question.)



- (a) Which orbit corresponds to the more massive star? How do you know?
- (b) Which velocity curve belongs to which star? How do you know?
- (c) Consider the points on the velocity curve marked below. Sketch the corresponding locations of the two stars on the orbits. Briefly explain your reasoning.



4.3. Consider the following eclipse light curve for a star. How many planets does the star have? What can you deduce about the relative sizes and orbital radii of the planets?



**4.4.** In a visual binary, we need to know the period ( $P$ ), angular extent of the semimajor axis ( $\alpha$ ), and distance ( $d$ ) to determine the star masses (see Sect. 4.2.2). Often the main source of uncertainty is  $d$ . If our measurement of the distance is  $d \pm \sigma_d$ , the fractional uncertainty is  $f_d = \sigma_d/d$ .

- If the fractional uncertainty in the distance is  $f_d$ , what is the corresponding fractional uncertainty in the total mass of the binary system?
- The brightest star in our night sky, Sirius, is a visual binary system. The brighter star has  $\alpha_A = 2.5''$ , the fainter star has  $\alpha_B = 5.0''$ , and the orbital period is 50.05 yr [23]. The distance to the Sirius system is  $2.64 \pm 0.01$  pc. What are the masses of Sirius A and B? What are the uncertainties in the masses?
- When we analyze stars orbiting the black hole at the center of the Milky Way (Sect. 3.2.1), we are essentially studying a visual binary with one really massive component. If our estimate of the distance to the center of the Milky Way is  $8.33 \pm 0.35$  kpc [24], what is the fractional uncertainty in our estimate of the black hole mass?

**4.5.** The binary system J0737–3039 has two pulsars orbiting with period  $P = 0.102$  day and eccentricity  $e = 0.088$  [25, 26]. It is nearly edge-on, and the velocity amplitudes are  $k_1 = 302.9 \text{ km s}^{-1}$  and  $k_2 = 324.5 \text{ km s}^{-1}$ . What are the masses of the two pulsars? What is the distance between the pulsars?

**4.6.** Imagine that an alien astronomer observes Jupiter transiting the Sun. For this problem, you may take Jupiter’s orbit to be circular and assume that Jupiter crosses the center of the star and does not emit any light itself. Define time  $t = 0$  to be the middle of the eclipse.

- Plot the radial velocity curve the alien astronomer would measure, spanning at least one period. Be quantitative; label the axes with appropriate units.
- Plot the eclipse light curve. Make sure to identify all phases of the eclipse and quantify when each phase starts and ends. Also specify the depth of the eclipse (as a fraction of the uneclipsed brightness of the Sun).

**4.7.** Show that the geometric probability for having a system oriented so that we see a transiting planet is  $P \approx R_*/a$  where  $R_*$  is the radius of the star and  $a$  is the orbital separation. Hint: use a geometric argument similar to the one in Sect. 4.3.1.

**4.8.** The Kepler space mission is searching for Earth-like planets using the transit technique.

- (a) Kepler is observing about 100,000 stars. If every one is just like the Sun, with an Earth orbiting at 1 AU, how many would show transits? Use the probability from Problem 4.7
- (b) Imagine that Kepler discovers a system that is an exact analog to our Solar System: “New Earth” orbiting “New Sol.” How deep is the transit? How long does each transit last? Assume the planet crosses the center of the star.
- (c) The reactionary group Just One Earth disputes the notion that “New Earth” is a planet and argues that it is a white dwarf instead. A white dwarf is about the same size as Earth but much more massive ( $M_{\text{WD}} \approx 0.6 M_{\odot}$ ). Calculate New Sol’s radial velocity amplitude for the cases in which New Earth is (i) a planet, or (ii) a white dwarf. (Keep the orbital period the same.)
- (d) We can now make radial velocity measurements with uncertainties of about  $40 \text{ cm s}^{-1}$ . Could we tell whether New Earth is a planet or a white dwarf?

**4.9.** Kepler has found some planets that orbit binary star systems. The presence of two stars complicates the motion (see Chap. 6), but not too much if the planetary orbit is large compared with the stellar orbits. (In this problem, assume the stars and planet all move in the same plane.)

- (a) Consider a coordinate system with the binary center of mass at the origin and the two stars on the  $x$ -axis. Let the semimajor axis of the binary orbit be  $a_{\text{star}}$ . Use a Taylor series expansion to show that the gravitational potential far from the stars can be written in polar coordinates  $(r, \phi)$  as

$$\Phi \approx -\frac{G(M_1 + M_2)}{r} - \frac{GM_1 M_2}{M_1 + M_2} \frac{a_{\text{star}}^2}{r^3} \frac{1 + 3 \cos 2\phi}{4} + \mathcal{O}\left(\frac{1}{r^4}\right) \quad (4.29)$$

- (b) Equation (4.29) indicates that a circumbinary orbit will be approximately Keplerian, with deviations that scale with the ratio  $(a_{\text{star}}/a_{\text{planet}})^2$  where  $a_{\text{planet}}$  is the semimajor axis of the planetary orbit (in the Keplerian approximation). Compute this ratio for the Kepler-16 system [13]. The two stars have velocity amplitudes  $13.7$  and  $46.5 \text{ km s}^{-1}$ , and their orbit has period  $41.1$  day and eccentricity  $0.16$ . The planet has a nearly circular orbit with period  $228.8$  day.

## References

1. Wolfram Research, Inc., *Mathematica*, 8th edn. (Wolfram Research, Champaign, 2010)
2. G.W. Marcy, R.P. Butler, E. Williams, L. Bildsten, J.R. Graham, A.M. Ghez, J.G. Jernigan, *Astrophys. J.* **481**, 926 (1997)
3. M. Mayor, D. Queloz, *Nature* **378**, 355 (1995)
4. R.P. Butler, J.T. Wright, G.W. Marcy, D.A. Fischer, S.S. Vogt, C.G. Tinney, H.R.A. Jones, B.D. Carter, J.A. Johnson, C. McCarthy, A.J. Penny, *Astrophys. J.* **646**, 505 (2006)

5. G.W. Henry, G.W. Marcy, R.P. Butler, S.S. Vogt, *Astrophys. J. Lett.* **529**, L41 (2000)
6. D. Charbonneau, T.M. Brown, D.W. Latham, M. Mayor, *Astrophys. J. Lett.* **529**, L45 (2000)
7. T.M. Brown, D. Charbonneau, R.L. Gilliland, R.W. Noyes, A. Burrows, *Astrophys. J.* **552**, 699 (2001)
8. G. Torres, J.N. Winn, M.J. Holman, *Astrophys. J.* **677**, 1324 (2008)
9. M. Mayor, D. Queloz, *New Astron. Rev.* **56**, 19 (2012)
10. C. Lovis et al., *Astron. Astrophys.* **528**, A112 (2011)
11. T. Barclay et al., *Nature* **494**, 452 (2013)
12. J.J. Lissauer et al., *Nature* **470**, 53 (2011)
13. L.R. Doyle et al., *Science* **333**, 1602 (2011)
14. W.F. Welsh et al., *Nature* **481**, 475 (2012)
15. N.M. Batalha et al., *Astrophys. J.* **729**, 27 (2011)
16. D. Charbonneau, T.M. Brown, R.W. Noyes, R.L. Gilliland, *Astrophys. J.* **568**, 377 (2002)
17. J. Harrington, B.M. Hansen, S.H. Luszcz, S. Seager, D. Deming, K. Menou, J.Y.K. Cho, L.J. Richardson, *Science* **314**, 623 (2006)
18. H.A. Knutson, D. Charbonneau, L.E. Allen, J.J. Fortney, E. Agol, N.B. Cowan, A.P. Showman, C.S. Cooper, S.T. Megeath, *Nature* **447**, 183 (2007)
19. S. Seager, D. Deming, *Annu. Rev. Astron. Astrophys.* **48**, 631 (2010)
20. W.J. Borucki et al., *Astrophys. J.* **745**, 120 (2012)
21. W.J. Borucki et al., *Science* **340**, 587 (2013)
22. T. Barclay et al., *Astrophys. J.* **768**, 101 (2013)
23. D. Benest, J.L. Duvent, *Astron. Astrophys.* **299**, 621 (1995)
24. S. Gillessen, F. Eisenhauer, S. Trippe, T. Alexander, R. Genzel, F. Martins, T. Ott, *Astrophys. J.* **692**, 1075 (2009)
25. M. Burgay et al., *Nature* **426**, 531 (2003)
26. M. Kramer et al., *Science* **314**, 97 (2006)